Available online at www.sciencedirect.com
ScienceDirect
Carbohydrate Research 342 (2007) 1223–1237
Carbohydrate RESEARCH

Linkage and pyranosyl ring twisting in cyclodextrins

Alfred D. French* and Glenn P. Johnson

Southern Regional Research Center, US Department of Agriculture, 1100 Robert E. Lee Blvd., New Orleans, LA 70124, United States

Received 9 November 2006; received in revised form 22 February 2007; accepted 23 February 2007
Available online 2 March 2007

Abstract—Acylated β-cyclodextrins (β-CDs) were studied to gain perspective on maltose octapropanoate, the crystal structure of which was reported in the preceding paper in this issue. Acylated β-CDs are distorted so we looked at other CDs and gained increased understanding of distortion in CDs and possibly, shapes in starch. Classic CDs have six to eight glucose residues in a doughnut shape that is stabilized by a ring of inter-residue O3···O2′ hydrogen bonds. On a ϕ,ψ energy map for a maltose analog that does not form hydrogen bonds, classic CD linkages have higher energies than structures that are stabilized by the *exo*-anomeric effect. In distorted β-CDs, which lack hydrogen bonding, some linkages attain low-energies from the *exo*-anomeric effect and acyl stacking. Those linkages result in left-handed helical geometry so other linkages are forced by the CD macrocycle to have counter-balancing right-handed character. Permethylated γ-CDs have two 'flipping' linkages as do some larger native CDs. Flipping linkages allow two left-handed segments to join into a macrocycle, thus avoiding the higher-energy, right-handed forms. Some glucose rings in derivatized β-CDs have substantial positive twists of the pseudo torsion angle O1–C1···C4–O4, adding right-handed character to balance the left-handed linkages. In substituted γ-CD, all residues have negative twists, giving extra left-handed character to the short, pseudo-helical segments. In non-macrocyclic molecules the twists ranged from −14° to +2°, averaging −6.1°. In these β- and γ-CDs, the twists ranged from −22° to +16° for $^4C_1$ rings, and the $^OS_2$ ring in acetylated β-CD has a twist of +34°. Glucose residues in other CDs were less twisted.
Published by Elsevier Ltd.

Keywords: Carbohydrate; Conformation; Schardinger dextrin; Crystal structure; Cycloamylose; CA; Computation; Hexaose; Heptaose; Octaose

1. Introduction

This work grew out of comparisons of related acylated compounds with our crystal structure of maltose octapropanoate (**1**) that is described in the preceding paper in this issue.[1] Besides the non-macrocyclic molecules covered in that work, we examined the acetyl-, propanoyl-, and butanoyl-β-cyclodextrins (β-CDs)[2] from the literature. β-CDs are macrocycles of seven α-(1→4)-linked glucose residues. They are part of a family of compounds that includes molecules with five[3] to 10 glucose residues,[4] typically produced by the action of cyclodextrin glucosyltransferase from *Bacillus macerans* on starch. CD names with Greek letters start with the six-residue α-CD; the cyclopentaose is synthetic and was not known when the nomenclature was developed. The family also includes molecules with many more residues per cycle. Because of the larger size, they are often called cycloamylose (CA), with a number denoting how many glucose residues are linked. CDs and CAs are important[4] in their own right because they can sequester guest molecules in their internal cavities[5] and can function as adsorbents or time-release agents. Since the beginning,[6] however, crystal structures of CDs and now CAs[7] have also been appreciated for their implications for the physical structures of polysaccharides, especially amylose, the mostly linear, α-(1→4) glucans that are components of most starches.

Our observations on the acylated β-CDs led us to examine other crystalline CDs and CAs, and report our findings in the present paper. Many specific structural explanations for the particular shapes of CDs have already been provided in the original papers or in previous reviews.[8,9] For example, particular hydrogen bonds or van der Waals interactions with guests can be

* Corresponding author. Tel.: +1 504 2864410; fax: +1 504 2864419; e-mail: afrench@srrc.ars.usda.gov

0008-6215/$ - see front matter Published by Elsevier Ltd.
doi:10.1016/j.carres.2007.02.033

important in determining the CD shape. Both channel- and cage-type crystal packing occur, and their different hydrogen bonding patterns distort the macroring in different ways.[9] General influences include tendencies to reduce the unoccupied volume of the cavity and to reduce the large glycosidic bond angles of CDs having the classic 'doughnut' or 'truncated cone' shape.[9] Novel contributions here include placing the geometries on an energy map for a maltose analog to learn about intrinsic forces other than hydrogen bonds that shape CDs. Also, we have examined the twisting of glucopyranosyl rings as a structural variable. A third unusual feature of the present work is our analysis of CDs in terms of helical characteristics. Although helices with six residues per turn are known for CA26,[7] we have found it useful to describe other CDs and CAs as being composed of helical segments.

In the following, our nomenclature and approaches constitute Section 2. We then show our analog energy map with our selected, crystallographically observed linkage conformations plotted. After that we consider examples of α-, β-, γ-, and ε-CD in detail. In the case of acylated β-CDs, we also examine the acyl stacking first described in Ref. 1. Before concluding, we look at the structural role and energy variation due to twisting of the glucopyranosyl rings.

2. Methods

2.1. Nomenclature

Figure 1 shows the crystallographically determined structures of MALTOS11[10] and α-maltose (MALTOT),[11] maltose being a really short amylodextrin. The atom numbering is shown as are the two types of inter-residue O3···O2′ hydrogen bonding found in many CDs. Also shown are the linkage torsion angles ϕ(O5′–C1′–O4–C4) and ψ(C5–C4–O4–C1′), often mentioned as the primary variables of oligosaccharide structure and a primary focus of the present work. We use $\phi_{O5'}$ and ψ_{C5} herein instead of the torsions defined with the hydrogen atoms attached to C1′ and C4, because hydrogen atoms are often poorly located by X-ray diffraction studies. Values of ϕ in the vicinity of 60° are described as conformations that benefit from the *exo*-anomeric effect[12] without intending to exclude other factors that stabilize that orientation.

Even though differences in geometry are visible for these two maltose structures (note the positions of O4′, for example), the substantial variability of the glucopyranose geometry in small crystalline di- or oligosaccharides is usually without obvious long-range consequences. However, the shapes of CD macrorings are inextricably linked with the shapes of the constituting pyranosyl rings. Models of CDs or a known amylose

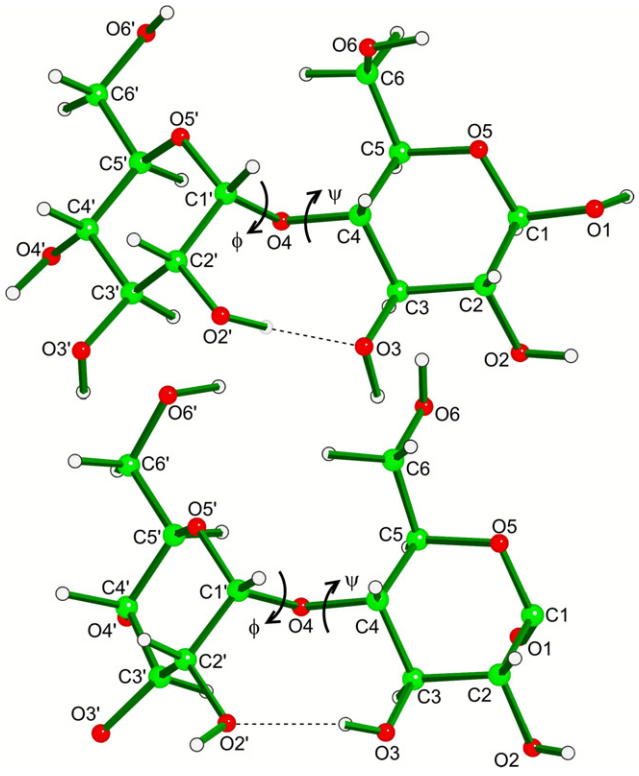

Figure 1. Maltose molecules from the MALTOT (lower) and MALTOS11 (upper) crystal structures. The MALTOT structure is for α-maltose, indicated by the axial oxygen atom on C1, where MALTOS11 is β-maltose monohydrate, with an equatorial O1. Both structures have an inter-residue hydrogen bond between O3 and O2′, but the direction is different. The bonds for the ϕ and ψ torsion angles are shown. Some hydrogen atoms for MALTOT were not located well and are not shown. Even though the structures have the same relative orientations based on the positions of the linkage atoms, there is a substantial difference in the position of the O4′ atoms. The distances between O4 and O4′ are 4.05 Å (MALTOT) and 4.41 Å (MALTOS11). Other differences include the orientation of the O6 groups.

shape constructed with just any glucopyranosyl geometry would usually be rejected because of too-short, inter-atomic contacts or unlikely glycosidic bond angles.

Previously,[13] we identified the O1···O4 distance (Fig. 2) as a simple descriptor of the various monomeric shapes needed to build models of different known CD and amylose structures. Although pyranose ring shapes are described more completely with three puckering parameters,[14] $d_{O1\cdots O4}$ values are often reported in crystal structure studies of CDs and CAs. Short values are found in classic CDs having small numbers of residues per cycle, and long distances are associated with larger numbers of residues per cycle.[8] CDs that are elliptical because of a flat inserted guest, such as *p*-nitrophenol,[15] have short O1···O4 distances for residues with O1···O4 virtual bonds that are parallel to the short axis, and long distances for residues that are parallel to the long axis.

Variation in $d_{O1\cdots O4}$ mostly results from systematic changes in the pyranosyl ring torsion angles,[16] and

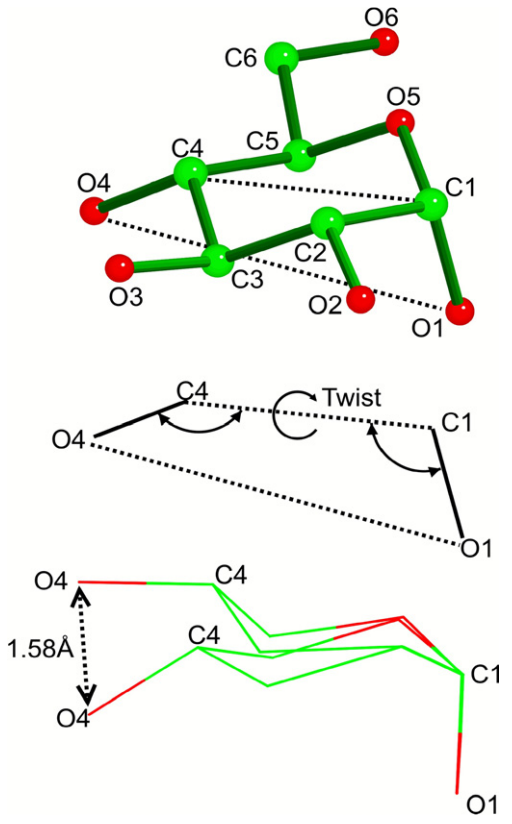

Figure 2. A glucose ring, without hydrogen atoms. Shown are the virtual bonds, C1···C4 and O1···O4, the pseudo angles O1–C1···C4 and O4–C4···C1; and the ring twist angle discussed in this paper, the pseudo torsion angle, O1–C1···C4–O4. Also shown are long and short glucose rings from KOYZAZ and MALTOT, superimposed on their C1–O1 bonds and rotated about that axis so that the distance between O4 atoms is minimized.

relationships with potential energy and puckering parameters are proposed.[17] When modeling CDs and amylose,[16] variations in this distance have large effects, partly because $d_{O1\cdots O4}$ correlates with the sums of the intra-residue pseudo angles, O1–C1···C4 and C1···C4–O4 (see Fig. 2). These angles, and $d_{O1\cdots O4}$ itself, determine the relative locations and orientations of successive residues. At the bottom of Figure 2, two glucose rings are shown with their C1–O1 bonds superimposed. The two rings, from panose (KOYZAZ)[18] and α-maltose[11] were chosen for their long and short $d_{O1\cdots O4}$ values, 4.78 Å and 4.06 Å, respectively. The positions of the O4 atoms differ by 1.58 Å. Glucose residues attached to these O4 atoms would be in quite different locations, and differences would accumulate with successive additions of the same glucopyranosyl ring geometries.

In this work, we use $d_{O1\cdots O4}$ as an indicator of stress in the glucopyranosyl ring as well as a characterization of local distortion of the CD. A related descriptor, the pseudo torsion angle, O1–C1···C4–O4, or glucopyranosyl ring twist, is shown in Figure 2. Previously, we had assumed that it does not differ importantly from 0°, but we now see a substantial range that is especially pertinent for CD structures.

2.2. Approaches

X-ray and neutron diffraction crystal structures were taken from the Cambridge Structural Database (CSD).[19] The structures are referred to with 'Refcodes' from the CSD to aid lookup and to specify which structure is being discussed; the specific structures have long names and journal articles often cover more than one structure.

The ϕ and ψ values of the CDs were placed on a previously published HF/6-31G(d) potential energy surface for a simplified maltose analog.[20] This analog has all hydroxyl groups replaced with hydrogen so that no conventional hydrogen bonding can occur. Unlike energies computed for native disaccharides with electronic structure theory (quantum mechanics, or QM), which are very dependent on the level of theory,[21] energies for these analogs are not.[22] Using an analog has advantages in addition to increased confidence in the energies obtained with a moderate level (faster) QM calculation. Calculations for analogs are faster because there are fewer atoms but more importantly, because there are no rotatable exocyclic groups. Assuming that the normal chair form of the ring is always a good starting shape, only one analog map is needed. With rotatable groups, the time needed is proportional to the number of combinations of exocyclic group orientations to be considered; each combination must have its own map so that the lowest possible energy can be determined at each point of the final adiabatic map.[23] Finally, at least for our present purposes, using an analog puts the energies of the backbones of the CD structures on an even footing regardless of whether the CD can make hydrogen bonds or not. (Energy surfaces for maltose itself that include the influence of hydrogen bonding were presented in Ref. 1.)

Our approach also includes characterizing the inter-residue linkage conformations of the various CDs in terms of the parameters of the amylose helix that would result if the specific glycosidic linkage geometry were repeated. The helix parameters are n, the number of residues per helix turn and h, the rise (or advance) per residue. By convention, right-handed helices are indicated by positive values of n, and left-handed helices have negative values. Describing local distortions of CDs in terms of helices is useful because the net value of h for a macrocycle, such as a classic CD, must be zero. When a local distortion of the CD occurs that would lead, if repeated, to a helix with an h value other than zero, there must be a compensating distortion that would lead to a comparable h value but opposite helix handedness from the initial distortion. As we will see below (Section 3.3), this requirement does not apply to

CDs that have 'flipping' linkages, and other exceptions could also occur.

In Ref. 1, we precisely determined n and h for each disaccharide residue and linkage using a spreadsheet.[24,25] We have also used it here to illustrate a few key points, but what we mainly want here is to know whether a linkage's ϕ and ψ values would lead to a right- or a left-handed helix. Therefore we used the spreadsheet to construct a ϕ,ψ to n–h conversion map. Those calculations were based on the non-reducing ring coordinates and glycosidic bond angle from β-maltose monohydrate[10] (MALTOS11) with all combinations of ϕ and ψ. Only the contour for $h = 0$ from that map was used here. It divides ϕ,ψ space into two regions, where left- or right-handed helices would occur. In this work we will refer to a sequence of glucose residues as pseudo-helical if its linkages are either all left-handed or all right-handed.

3. Results and discussion

The QM energy map for 360° of rotations of the ϕ and ψ torsion angles of our maltose analog is shown in Figure 3. There are two significant minima and four principle maxima. The minima are separated by a low saddle point at $\phi = 80°$, $\psi = -250°$; both minima have ϕ values that are consistent with the *exo*-anomeric effect. Points are plotted on the map that correspond to the ϕ and ψ values in crystal structures of the CDs in this work. Also shown are four reference points. One is the location of ϕ and ψ for maltose octapropanoate (**1**),[1] and one is from the linkage in MALTOS11.[10] The point for **1** indicates a geometry favored[1] by maltose linkages when an inter-residue hydrogen bond is not found, and MALTOS11 was selected because it is an accurately determined example of a strongly hydrogen bonded structure. Two other points represent the nearly identical averages of 663 linkages from α-CDs ($\phi = 108.9°$ and $\psi = -111.4°$) and from 1325 linkages from β-CDs ($\phi = 110.4°$ and $\psi = -112.2°$). That survey excluded linkages between substantially distorted $^4C_1$ and non-chair shapes.

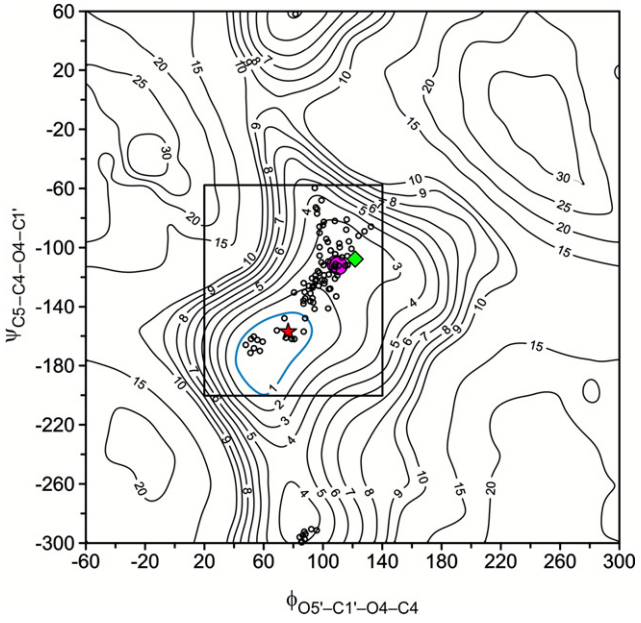

Figure 3. A ϕ,ψ energy surface computed with HF/6-31G(d) electronic structure theory for a maltose analog that lacks all hydroxyl groups. The ϕ and ψ values found in crystal structure determinations of the selected cyclodextrins are plotted, as are four special landmarks: the location of ϕ and ψ for maltose octapropanoate (★); the linkage in MALTOS11 (♦); and two partly overlapped ● symbols that represent the average conformations of 663 linkages from α-CDs and for 1325 from β-CDs. The rectangle delineates the area of the map to be shown in discussions of the individual CDs, and the four landmark points are shown each time. If ϕ_H and ψ_H had been used, the axes would range from −180° to 180°.

An inset rectangle in Figure 3 marks the region of the primary minimum that will be enlarged and shown for each size of CD, along with the four landmark points mentioned above. The nine points in the secondary minimum (including one point in the part of the minimum that is at the top of the map) are tightly grouped, close to the minimum and have corresponding energies of just under 4 kcal/mol. Although they correspond to dramatic changes in the CD structure, there is little else to say about these points relative to the map. Eight points in the edge-of-the-map minimum are from the four molecules in permethylated γ-CD and one is from the asymmetric unit of ε-CD that consists of half a molecule.

3.1. α-CDs

In the α-CD–cyclopentanone complex crystal[26] (KIRJOK10), there are two different CD rings. One, shown in Figure 4 without hydrogen atoms, has sixfold rota-

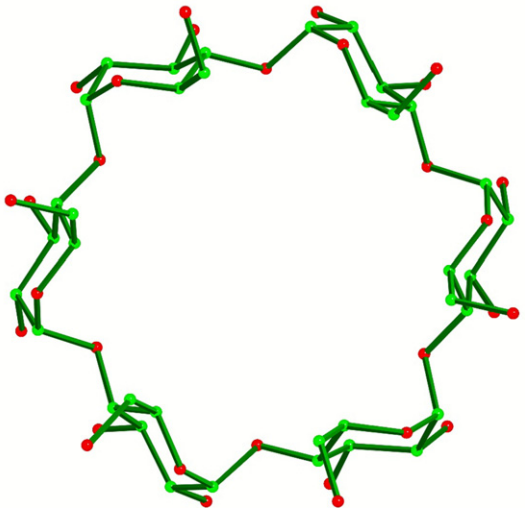

Figure 4. The 6-fold symmetrical KIRJOK10 α-CD. Hydrogen atoms, water molecules and the disordered cyclopentanone guest are not shown.

tional symmetry, and one has threefold symmetry (not shown). The CD in Figure 4 has the quintessential classic structure, with complete O3···O2′ hydrogen bonding. Because of the symmetries, there are only three independent linkage and ring geometries. All three ϕ,ψ points are within a few degrees of the overall averages, while the ring twists are slightly positive in all three residues: 1.3° for the molecule with sixfold symmetry, and 1.9° and 2.0° for the molecule with two unique geometries. The O4···O4′ distances are 4.26 Å, 4.23 Å, and 4.26 Å, respectively.

The limited energy map with the locations of the KIRJOK10 structures is shown in Figure 5. Not only do these structures fall on top of the average CD points, but they also are essentially on the dashed $h = 0$ line (see Section 2.2). All three linkages correspond to about 2.5 kcal/mol on the analog map, plausible because the analog has no hydrogen bonding. The strong hydrogen bonds ($d_{O3\cdots O2'} = 2.82$ Å for the molecule with sixfold symmetry) could overcome the stress when the backbone atoms are in this arrangement; the enthalpy of stabilization from a hydrogen bond in water is about 5.5 kcal/mol.[27]

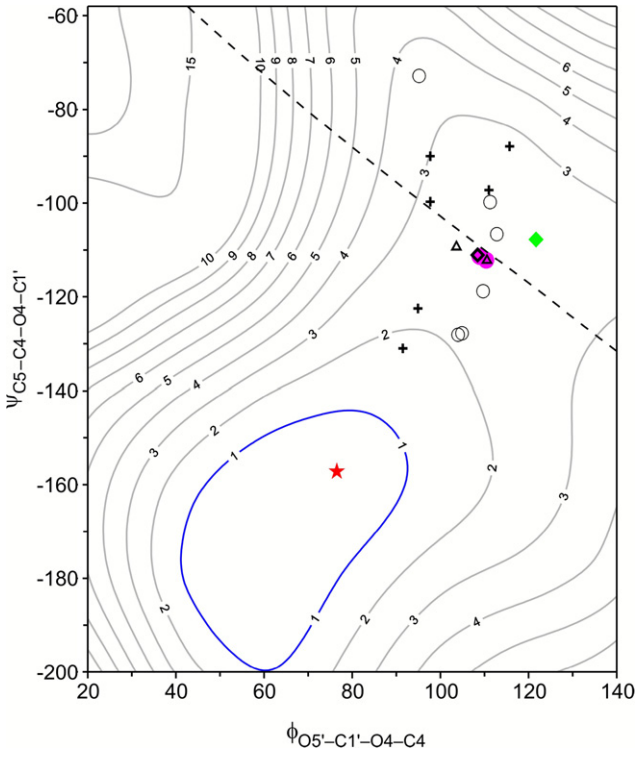

Figure 5. Small energy surface with linkage geometries from KIRJOK10 and CHXAMH03 (○) indicated. The linkage from the CD with 6-fold symmetry from KIRJOK10 is shown by ◇, and △ indicates the threefold structure's linkages. This surface was calculated using $\phi_{O5'\text{–}C1'\text{–}O4\text{–}C4}$ and $\psi_{C5\text{–}C4\text{–}O4\text{–}O1'}$. If ϕ_H and ψ_H had been used, the axes would range from −100° to 20°, and −80° to 60°, respectively. Also shown as + are the linkage geometries from the permethylated α-CD, TEVCEC structure. The dashed line indicates linkage geometries that, if extrapolated into amylose helices, would have an h value (advance per residue along the helix axis) of 0. Linkages above the line correspond to right-handed helices, and those below would be left-handed. Other (landmark) points are as described in the caption for Figure 3.

The linkages from a hydrated, but otherwise empty, α-CD (CHXAMH03)[28] depicted in Figure 6 are also shown in Figure 5. It is substantially distorted; one residue leans inward to donate its O6 hydroxyl hydrogen to a water molecule in the CD's cavity. One linkage falls near the 4 kcal/mol contour; and the others are somewhat spread out. However, the average ϕ and ψ values are close to the overall average. Compared to the KIRJOK10 linkages above, three CHXAMH03 linkages have higher-energy, and three have lower-energy. The higher-energy structures fall on the right-handed side of the $h = 0$ line, and the lower-energy structures fall on the left-handed side. The ring twist values are +5.4°, −4.8°, −2.6°, −0.4°, −2.6°, and −3.5°, and $d_{O4\cdots O4'}$ ranges from 4.16 Å to 4.42 Å.

Permethylated α-CD, TEVCEC[29] is shown in Figure 7. Ring twists in this molecule range from −4.4° to +3.6°, similar to those in CHXAMH03. The ϕ and ψ torsion angles (Fig. 5) also have a general similarity to those of the CHXAMH03 structure, and none is very far from the average value. Two of the points from TEVCEC have slightly lower-energy than the average CD points, four points are slightly higher. The $d_{O4\cdots O4'}$ ranges from 4.10 Å to 4.47 Å.

The linkage geometries for all of these α-CDs are in a region of our analog map where calculated energies are greater than 1 kcal/mol, regardless of whether hydroxyl

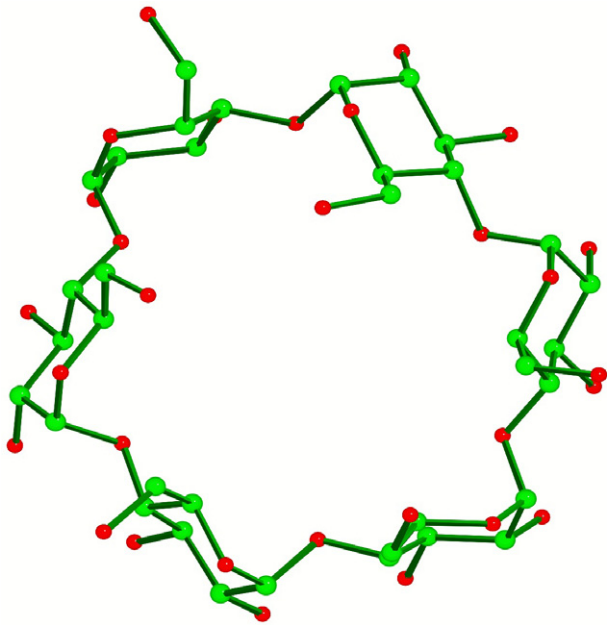

Figure 6. Drawing of the distorted CHXAMH03 α-CD. The residue in the 1:00 o'clock position is leaning into the cavity so that the O6 can hydrogen bond to a water molecule in the cavity, not shown. The residue in the 11:00 o'clock position is leaning outwards. O3···O2′ hydrogen bonding is disrupted only between these two residues.

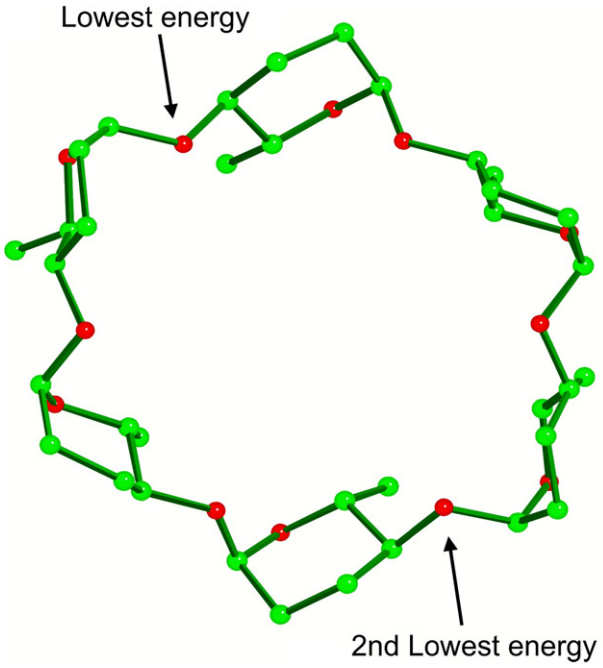

Figure 7. Methylated α-CD, TEVCEC. All atoms except the ring, O4 and C6 atoms have been deleted for clarity. The linkages with low energy in Figure 5 are indicated.

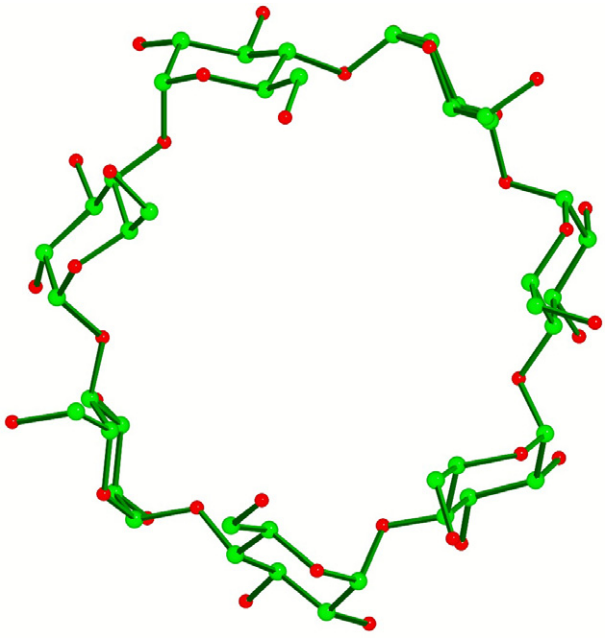

Figure 8. The BUVSEQ03 β-CD, hydrogen atoms not shown. This molecule exhibits a normal range of tilting of the glucose residues toward the center of the molecule. Continuous O3···O2′ hydrogen bonding is found for this structure.

groups or methoxy groups are present. Still, there is enough conformational flexibility that the nearly cylindrical shape of the symmetrical hydroxyl-bearing KIRJOK10 structure can morph into a bowl-like shape for the permethylated TEVCEC molecule.

3.2. β-CDs and acyl stacking

Because no crystal space group has sevenfold rotational symmetry, the seven glucose residues of β-CDs will not be identical in crystal structures. The deutero-β-cyclodextrin undecakis (deuterium oxide) clathrate, BUVSEQ03, at 120 K[30] is shown in Figure 8. Its ring twists have a limited range, −1.0°, +0.7°, +1.2°, −2.5°, +1.2°, +4.9°, and −1.5°. Hydrogen (deuterium) bonding is found all around the CD. The SIGHOF structure of β-CD[31] (not shown) is also deuterated, with ethanol and water guests. O3···O2′ hydrogen (deuterium) bonding is also maintained around its macroring, with shorter distances between the O3 and O2′ atoms than in BUVSEQ03. Values of O4′–C4′···C1′–O4 range from −5.0° to +6.3°. Figure 9 is the limited energy map with the linkage geometries from the BUVSEQ03 and SIGHOF crystal structures. Both sets of ϕ,ψ values have comparable, narrow ranges that average to values near the overall CD averages. Given the impossibility of crystallographic symmetry for β-CD, these structures would be considered to have the classic shape.

The backbone of the quite-distorted, permethylated β-CD, HEZWAK01[29] is shown in Figure 10. A unique

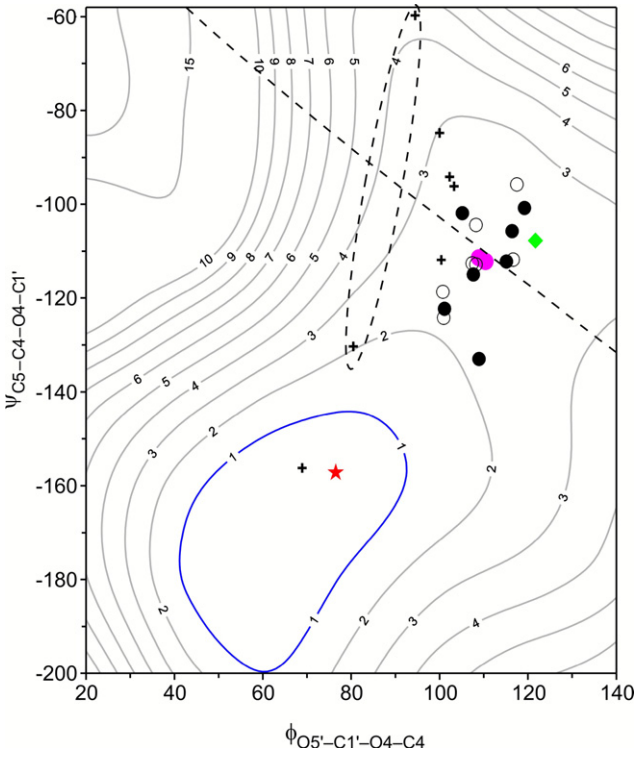

Figure 9. Small energy surface with linkages from BUVSEQ03 (○), SIGHOF (●) and HEZWAK01 (+). The dashed-line ellipse contains the linkages that connect to the $^1C_4$ ring in the permethylated β-CD. The di-equatorial linkage is lower and closer to the linkage in **1** shown by the ★.

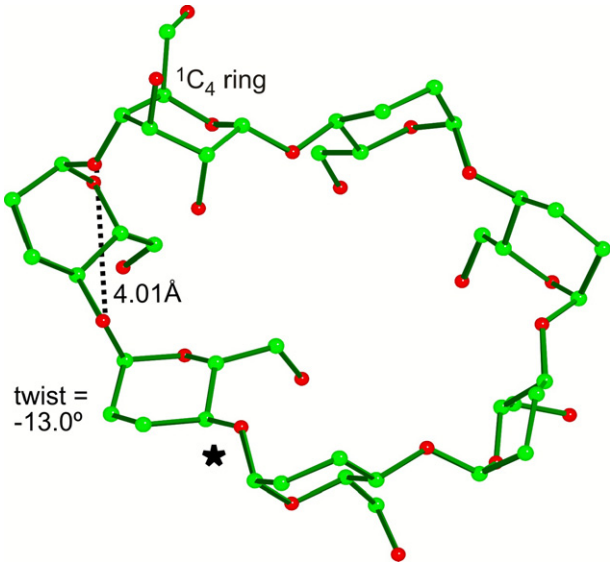

Figure 10. The permethylated β-CD molecule (HEZWAK01), showing the $^1C_4$ ring and the residue with a large, right-handed twist. The ★ indicates the linkage having a conformation close to that in **1**.

feature of this molecule is its $^1C_4$ glucose ring, which has a twist of +13.8°. Moving counter-clockwise from the $^1C_4$ ring around the macroring as drawn, the second glucose residue has a counteracting twist of −13.0°. Other twists are −0.1°, −6.2°, 4.0°, −0.1°, and 2.2°. The C4 end of the second ring is in a linkage with geometry very similar to that of **1**. Figure 9 also shows the ϕ,ψ points for HEZWAK01. All of the ϕ values are closer to 60° (favored by the *exo*-anomeric effect) than average ϕ values of SIGHOF or BUVSEQ03. One of the linkages to the $^1C_4$ ring is di-axial, and the other is di-equatorial, unlike the usual axial–equatorial arrangement. Those two linkages are inside the dashed-line ellipse in Figure 9, with the di-equatorial point lower and closer to the linkage in **1**. The energy contours of Figure 9 may be less relevant for these two linkages.[32] The authors of Ref. 31 point out that the O4 atoms on the $^1C_4$ ring and its neighbor to the right in Figure 10 make an O4″···O4′···O4 angle of 161.5°. Such an extended local arrangement, if repeated, would not be compatible with forming a small macrocycle. The two residues that are connected by the linkage with the star make a corresponding angle of 144.6°. Both of those angles are considerably straighter than the value for a symmetrical β-CD of (180° − 360°/7=) 128.6°. The residue that connects these two sequences has a short $d_{O1\cdots O4}$ of 4.01 Å.

The acetyl- (ICUFAN), propanoyl- (ICUFIV) and butanoyl- (ICUFOB) β-CDs[2] also have substantial distortions from the classic shape. These distortions were attributed[2] to the lack of O3···O2′ hydrogen bonds and a tilting of the glucose residues to relieve steric hindrance between adjacent acyl chains. In the cases of the nearly isomorphous acetate and propanoate, one of the glucose residues takes an $^OS_2$ shape. Earlier, Durette and Horton had proposed that the electronegativity of acyl groups shifted the conformational equilbria of monosaccharides toward the alternative $^1C_4$ shape.[33] The $^1C_4$ shape was seen for the permethylated HEZWAK01, above, but not, so far at least, for the acylated CDs. Figure 11 shows the propanoate structure with all exocyclic groups removed except for the carbonyl parts of the propanoate groups that are involved in the stacking interactions as discussed in Ref. 1. Those stacking interactions should give some extra stability to the linkages that allow their formation.

Figure 12 shows the seven ϕ,ψ points from each of the three acylated β-CDs on the limited energy surface. The smaller dashed-line oval surrounds the linkage

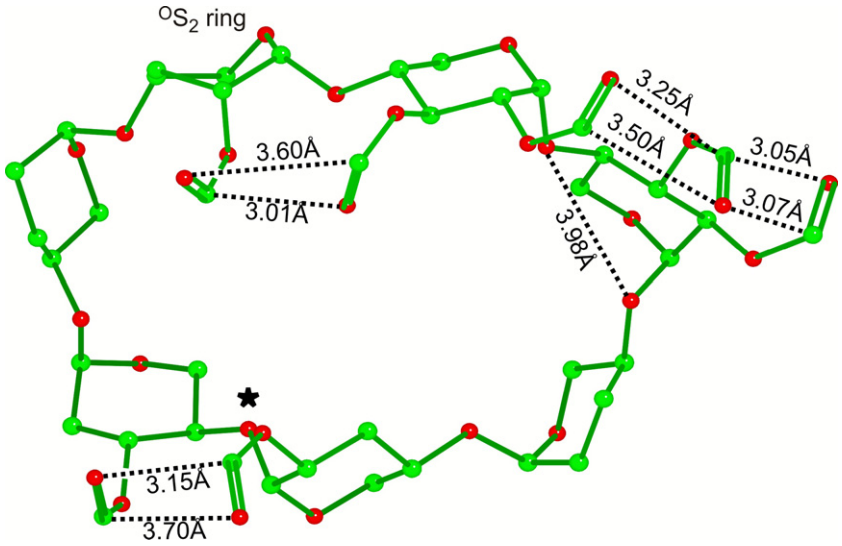

Figure 11. The propanoylated β-CD (ICUFIV), showing the $^OS_2$ ring and the acyl stacking discussed further in Ref. 1. All exocyclic groups have been removed, except for the carbonyl atoms involved in stacking interactions. ★ indicates the linkage having a conformation close to that in **1**.

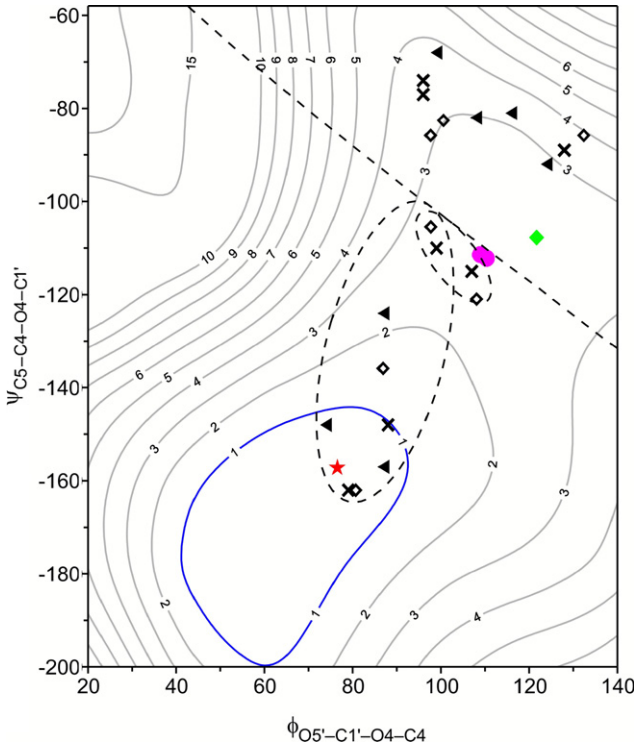

Figure 12. As in Figure 5, but with the linkage conformations from the acylated CDs. ×, ◇, and ◀ represent conformations in the β-CD acetate (ICUFAN), propanoate (ICUFIV) and butanoate (ICUFOB), respectively. The larger dashed-line oval contains the linkages that correspond to the stacked acyl groups as discussed in Ref. 1, while the smaller oval surrounds the linkages that are attached to $^{O}S_2$ rings.

geometries that connect the $^{O}S_2$ rings to their neighbors in the acetate and propanoate. Several ϕ,ψ points for the acylated β-CDs are close to **1**, and all points within the larger dashed oval have the stacking of the acyl groups. Both inter- and intra-residue stacking are shown in Figure 11 for the propanoate; the acetate is quite similar. One of the stacking interactions is across the linkage to the $^{O}S_2$ ring, and another includes three acyl groups, two of which are on one residue. In the acetylated β-CD, the glucose ring with intra-ring acyl stacking has the shortest $d_{O4\cdots O4'}$ of which we are aware, 3.88 Å; the distance for the corresponding ring in the propanoate, also with intra-ring acyl stacking, is 3.98 Å (Fig. 11). The sums of the indicated non-bonded carbonyl C to carbonyl O distances for these intra-residue stackings are smaller than for the inter-residue stackings. The third stacking in the acetate and propanoate spans the residues connected with a linkage having ϕ and ψ closest to **1**.

The accompanying paper[1] reported that the linkage geometry and non-reducing residue of **1**, when reproduced, result in a very extended, left-handed helix with $n = -4.63$ and $h = 3.99$ Å. Therefore, one might question how β-CD conformations near to **1** in Figures 9 and 12 can be part of a closed macrocycle. In part, the answer is that the average ϕ and ψ values for these derivatized β-CDs are still reasonably close to the all β-CD averages. The average ϕ torsion angle for each acylated structure is about 10° less, and the average ψ values for each structure are just 1.0° to 5.2° different from the all β-CD average values. The right-handed linkages above the $h = 0$ line compensate for the extended left-handed forms that result from the conformations inside the larger dashed oval. To illustrate this, we have calculated n and h values for two points having ψ values at the most right-handed limits of the data. Thus, a conformation with $\phi_{O5'\text{–}C1'\text{–}O4\text{–}C4} = 100°$ and $\psi_{C5\text{–}C4\text{–}O4\text{–}C1'} = -70°$ corresponds to a right-handed helix with $n = +8.26$ and $h = 1.42$ Å when made with the non-reducing ring from MALTOS11. When $\phi = 130°$ and $\psi = -90°$, n and h are +6.7 and 2.47 Å.

In addition to having some ϕ and ψ values that lead to compensating right-handed helical conformations, positive values of the within-residue, O4–C1′···C4′–O4′ pseudo torsion angle also bias multi-residue structures toward a right-handed helical twist, as described in Section 4. Thus, twists of the pyranosyl rings can also counterbalance the preference for left-handed shapes that results from the *exo*-anomeric effect and acyl stacking. In the case of the acetylated and propanoylated β-CDs, the $^{O}S_2$ rings provide a substantial twist. Their O4–C1′···C4′–O4′ torsion angles are +34° and +31°, respectively. The $^{4}C_1$ rings in the acetate have twists of −1.2°, −8.3°, 15.9°, −2.5°, −11.5° and 4.4°, while their propanoate counterparts have twists of 0.5°, −7.5°, 12.1°, 0.1°, −9.7°, and 5.5°.

The butanoyl-CD (Fig. 13) has a different space group and is not isomorphous with the acetyl- and propanoyl-CDs. Still, it is similar but somewhat less crumpled, probably because it self-complexes one of its butanoate chains.[2] All of its glucose rings have the $^{4}C_1$ shape, and the twist values are 4.1°, 1.8°, 3.7°, −11.1°, −1.3°, 10.9°, and −7.6°. Of these, only the 10.9° twist indicates substantial stress. Also, in keeping with the lower distortion, the shortest $d_{O4\cdots O4'}$ in this structure is 4.16 Å, considerably longer than the shortest distances in the other substituted β-CDs discussed above. Of the three linkages bridged by stacked butanoate groups, the one with the shortest inter-acyl distances has the most negative value of ψ. The stacking with the longest carbonyl oxygen to carbonyl carbon distances (marginal at 3.74 Å and 3.78 Å) corresponds to the least negative value of ψ in the large dashed ellipse in Figure 12. Two intra-residue stackings are present, both of which are also part of inter-residue stackings. The variable geometries and occurrence in these structures suggest that acyl stacking is a relatively weak, but still stabilizing, interaction. Two long $d_{O4\cdots O4'}$ values of 4.59 Å and 4.61 Å characterize the residues whose butanoate groups on C2 are stacked with the rings that have intra-residue stacking. In the propanoate, the longest $d_{O4\cdots O4'}$ for a $^{4}C_1$

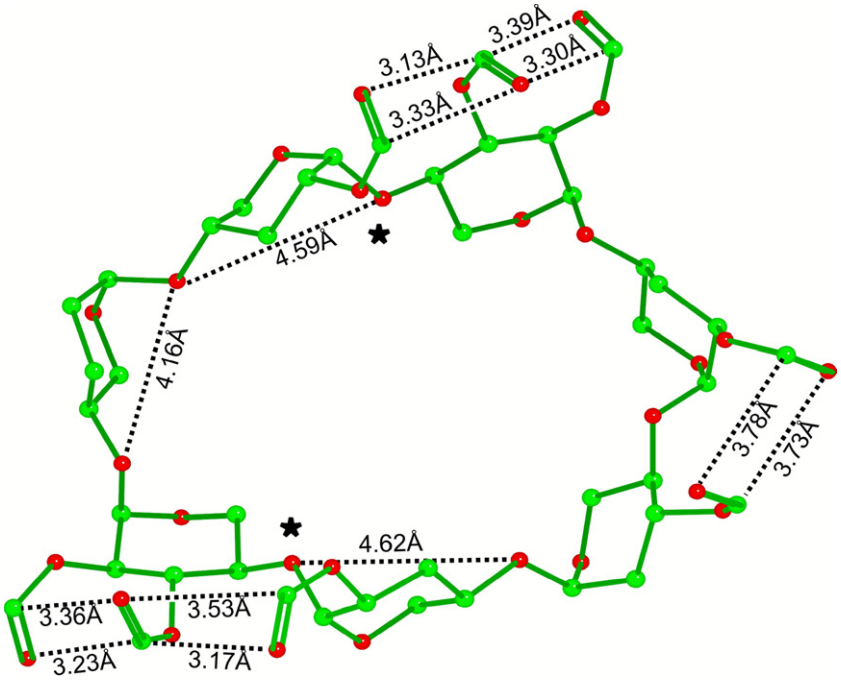

Figure 13. The butanoylated β-CD (ICUFOB), showing the acyl stacking. All exocyclic groups have been removed, except for the carbonyl atoms involved in stacking interactions. The ★s indicate the linkages having conformations close to that in **1**.

ring is 4.49 Å; the acetylated CD has one distance of 4.61 Å.

3.3. Permethylated γ-CD

One macroring of permethylated γ-CD,[34] BEBJAT, which has two flipping linkages in each of its four crystallographically independent molecules is shown in Figure 14. The flipping geometries are at the bottom or top of Figure 3 whereas the others are within its inset box. The flipping linkages result in a gross change in molecular orientation compared to the orientations from geometries in our central region of ϕ,ψ space. If amylose models were composed of only flipping linkages, they would have approximate twofold screw symmetry. In CA26 (not shown),[7] the molecular shape consists of two turns of a compressed left-handed helix with six residues per turn, connected by a 13th residue and a flipping linkage to two turns of an oppositely oriented helix. In turn, the second helix is connected by another flipping linkage and extra residue back to the first helix. In BEBJAT, one of the rings involved in the flipping linkage is followed by three 'normal' linkages, and then another flipping linkage occurs.

Each of the four molecules in the BEBJAT crystal is similar to the others, and all are generally similar to a permethylated γ-CD molecule in a different crystal structure with a lower level of hydration.[35] The six non-flipping linkages from each of the four BEBJAT molecules are indicated in Figure 15. The approximate twofold rotational symmetry for each molecule is indicated by the close proximity of open and filled symbols of the same type (see caption). Because these molecules have such similar structures, we think that this general shape for γ-CD is intrinsically preferred when inter-residue hydrogen bonding does not occur. When hydrogen bonds do occur, for example in the *n*-propanol clathrate hydrate (SIBJES),[36] the ϕ and ψ values of the γ-CD structure are essentially the same as in the KIRJOK10

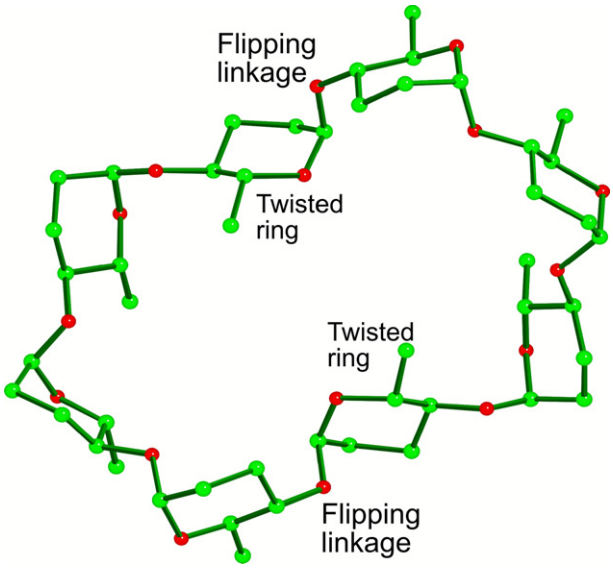

Figure 14. One of eight molecules of permethylated γ-CD, BEBJAT. Only the ring, O4 and C6 atoms are shown. The two twisted rings have O4–C1···C4–O4 torsions of −17° and −22°. The flipping linkages have conformations in the minimum at the bottom of Figure 3.

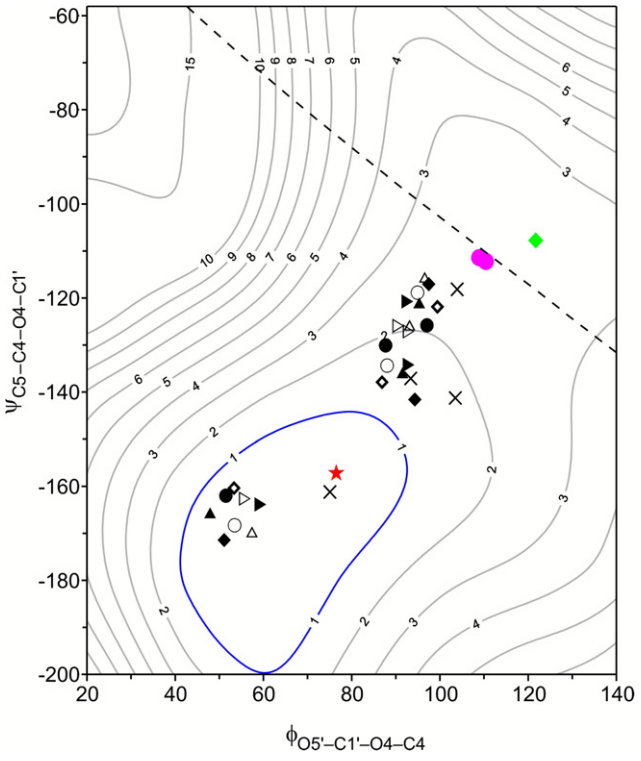

Figure 15. The same energy contours as in Figure 5, with the linkage conformations from the four molecules of permethylated γ-CD, BEBJAT. Each of the four molecules has pseudo twofold rotational symmetry. For each molecule, two of the linkages are in the secondary minimum with ψ values near −300° (Fig. 3). The remaining 24 BEBJAT linkage conformations are in two groups. Two linkages in each molecule are near $\phi = 50°$, and four are near $\phi = 90°$; linkages related by pseudo-symmetry are indicated by open and filled symbols. All ▶ and ▷, for example, represent different linkages from one of the four BEBJAT molecules. Also shown (×) are four linkage conformations from the ε-CD (NOBBOV02); its fifth, flipping linkage is in the secondary minimum (Fig. 3).

α-CD structure. SIBJES (not shown) has a classic shape with fourfold rotational symmetry.

Each flipping linkage corresponds to more than 3 kcal/mol in Figure 3, but it is plausible that a lower total energy is achieved by flipping and simultaneous decrease in other types of stress. In each of the BEBJAT molecules, there are two linkages that have even smaller ϕ values than in **1**, ranging from 48° to 59°. With ψ values ranging from −160° to −171° those eight points are also found within the 1 kcal/mol contour in Figure 15. The other non-flipping linkages also have a lower-energy than the average CD, and all of the ϕ,ψ points other than the flipping linkages correspond to left-handed geometries. The sequences of three linkages, all with left-handed twisting, correspond to a distorted helix.

As the number of glucose residues per CD increases, the methylated γ-CDs are the first to exhibit the flipping motif. Unlike β-CDs, they have an even number of residues per cycle, so it is possible to have two evenly spaced flipping linkages. Still, it is not surprising that in the case of γ-CD, there is substantial residue distortion required to essentially complete a helix turn plus a flip, in four residues. All ring twist values for BEBJAT are negative, with the smallest twist being −3°, and large negative ring twists are indeed found for these molecules. The eight rings whose C1 ends are involved in the flipping have twists from −12° to −22°. Based on models,[1] there is precedent for helices with fewer than four residues per turn; n values of −3.55 and −3.64 residues per turn were generated with geometries from the FOXSUG20[37] and MAPNEW[38] structures. Since those were the smallest values of n that we found, CDs with eight residues might be the smallest that can achieve a structure containing two flipping linkages.

3.4. Native ε-CD (CD10)

There are some close similarities between the NOBBOV02 structure of ε-CD[39] shown in Figure 16 and the BEBJAT γ-CD structure above. Both molecules have two flipping linkages. The NOBBOV02 crystal structure has only one unique molecule instead of four and actual, instead of pseudo, twofold symmetry. Therefore, there are only four points in Figure 15 for NOBBOV02. Still, the distribution of ϕ and ψ values is similar, despite the absence of hydroxyl groups in permethylated γ-CD and their presence in ε-CD. Again, all of the non-flipping linkages correspond to left-handed helix geometries with lower-energies than the average α- and β-CD geometries. The linkage geometry adjacent to the flipping linkage is very similar to that in **1**, with $\phi = 76.5°$ and $\psi = -161.4°$. Ring twists range from −2.3° to −13.5°, with the largest value for the ring whose C1 end is part of the flipping linkage. The second largest twist, −11.5°, is for the ring whose C4 end is part of the flipping linkage. These flipping linkages are stabilized by an O3···O6′ hydrogen bond that has a minor O3 ··· O5′ component as well. Three of the linkages are stabilized by O3···O2′ hydrogen bonds, but the linkage closest on the map to that of **1** is not. In Figure 15, the linkage for NOBBOV02 that is closest to the average α- and β-CD conformations has the shortest (strongest) O3···O2′ hydrogen bond.

4. The role of, and calculated energy for, ring-twisting

We view the role of the variable O4–C1′···C4′–O4′ torsion angle in determining the shapes of modeled polymers as a partner to the function of $d_{O4\cdots O4'}$, mentioned in Section 2.1. Variations in both affect the positions of subsequent glucopyranose residues in model CDs and amylose chains. Because they each have substantial variability, both substantially increase the flexibility of α-(1→4)-linked molecules compared to model molecules

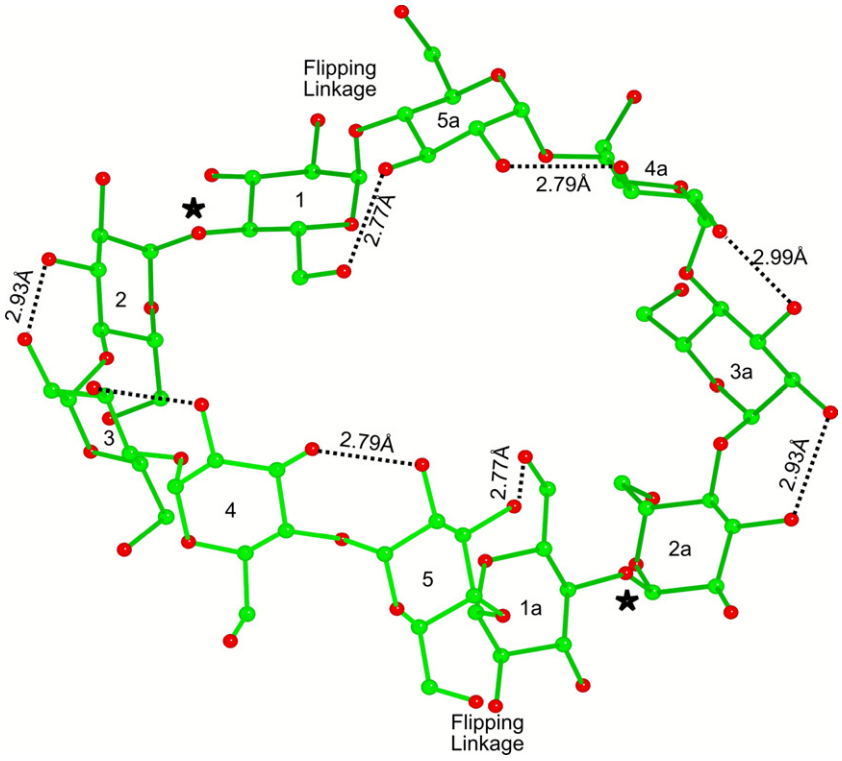

Figure 16. The molecule of ε-CD (NOBBOV02), showing the flipping linkages, the conformations similar to that in **1** (indicated by ★), and the hydrogen bonding. Glucose rings related by twofold rotational symmetry are numbered 1, 1a, etc.

that only vary ϕ and ψ. Table 1 shows the various patterns of twisting for the different structures that are mentioned herein and in the previous paper. Just as there are systematic relationships with CD structure for $d_{O4\cdots O4'}$, different types of structures seem to have different amounts of ring twist.

Among the non-macrocyclic structures listed in Table 4 of Ref. 1, only one residue, from erlose monohydrate (HAHXUJ),[40] has a positive twist, 2.4°. The others range from −0.5° to −14.4°, and the average value is −6.1°. Therefore, zero and positive twist values could be seen as distortions. All of the classic (α-, β-, and γ-) native CDs in Table 1 of the present paper have average twists that are essentially 0°, as do the substituted α- and β-CD $^4C_1$ rings. This distortion, on the average, from the non-macrocyclic average twist, can be seen as a consequence of being part of a macrocycle that lacks flipping linkages. The greater range of twists in the substituted β-CD rings parallels the greater range of ϕ and ψ values for those CDs, even when just considering the $^4C_1$ rings. With the introduction of flipping linkages in the substituted γ-CD, the average twist shifts to a value more negative than even that of the non-macrocyclic molecules. Native ε-CD and CA14[41] (NOBBUB) have progressively less twisted averages, but still all twists are negative. With some positive twists, CA26 still has a negative average, but the average is smaller. Perhaps this is in keeping with its helical segments that resemble classic α-CDs with zero twist and continuous inter-residue O3···O2′ hydrogen bonds. The helix turns of CA26[7]

Table 1. Glucopyranose ring twists, based on structures mentioned in text

Structure	Minimum twist value (°)	Maximum twist value (°)	Average (°)
Non-macrocyclic	−14.4	2.4	−6.1
Native α-CD	−4.8	5.4	−0.4
Permethylated α-CD	−4.4	3.6	−0.1
Native β-CD	−5.0	6.3	0.1
Substituted β-CD, $^4C_1$	−13.0	15.9	−0.6
Substituted β-CD, non-$^4C_1$	13.8	34.4	26.4
Native γ-CD	−4.4	3.0	0.3
Permethylated γ-CD	−22.1	−3.3	−10.4
Native ε-CD	−13.5	−2.3	−8.6
Native CA14	−10.5	−1.9	−4.8
Native CA26	−11.1	3.7	−2.6

correspond to a break in the macrocycle of α-CD and slight ($h = 1.3$ Å) extension.

A rough idea of the magnitude of the impact of residue twist on helix handedness can be gained by considering models made with ϕ and ψ set to the average values for β-CDs. By combining those torsion angles and a glucose residue with an average twist, the resulting model should be a cyclodextrin, that is, a helix with $h = 0.0$ Å. For example, a DUDXOP (methyl α-maltotrioside)[42] monomer with a nearly average −7.5° twist results in a very slightly left-handed helix with $h = 0.01$ Å. On the other hand, extrapolation of a HEGXOG (erlose trihydrate)[43] monomer with a twist of −14.4° creates a left-handed helix with $h = 0.62$ Å and −7.52 residues per turn, which combine to give a pitch of 4.7 Å. Another residue from HEGXOG has a smaller twist, −12.7°, but a 0.15 Å longer $d_{O1\cdots O4}$ of 4.60 Å. It gives a left-handed helix with $n = -9.33$ and $h = 0.72$ Å, for a pitch of 6.7 Å, again despite ϕ and ψ values that would on average lead to a macrocycle. A maltotritol (MENRAY)[44] residue with −0.5° gives a right-handed helix with $h = 0.31$ Å, and a HAHXUJ residue, with its twist of 2.4° gives a right-handed helix with $h = 0.38$ Å. With its positive 34° twist and other geometrical features, the $^{O}S_2$ ring from the acetylated β-CD gives a right-handed helix with $n = 7.00$ and $h = 3.50$ Å!

Energies for glucose rings in different twisted shapes were calculated with the empirical force field program MM4[45] and with B3LYP/6-31+G(d) density functional theory in the Jaguar 6.5 software package.[46] Facilities in these programs allow atoms to be held at a point (all three Cartesian coordinates held), on a line (two held coordinates) or in a plane (one held coordinate). The different shapes were created by fixing C4 at the origin, C1 on the x-axis, and O4 in the x–z plane, while O1 was stepped in 0.1 Å increments perpendicular to the x–z plane. Each increment corresponds to about 4.25° of twist. Figure 17 shows the various relative energy values obtained. These qualitatively similar results favored left-handed twists but the minimum energy values for the O4–C1′···C4′–O4′ pseudo torsion angle are about −10° while the experimental average value for non-macrocyclic compounds was −6.1°. The lower-energies were associated with twisting O1 toward O2. Similar calculations (not shown) with 2,5 dihydroxytetrahydropyran (organic nomenclature) gave a minimum with positive twist values, and so interaction is likely between O1 and O2 (carbohydrate nomenclature) in glucopyranose. The calculations on glucose suggest that the loss of the $^{4}C_1$ shape may occur when other forces in the ring require a substantial right-handed twist in the structure. Since the calculated energy rises rapidly when the $^{4}C_1$ glucose ring is twisted to the right, it can quickly reach levels where other ring forms have lower-energy.

Figure 18 shows every other twisted ring from the B3LYP calculations. Note that the C1···C4 distance remained constant. The O4 atom was in motion within the x–z plane, but the ring atoms other than C1 and C4 moved substantially more, especially C2 and C3. Although the $^{4}C_1$ designation still applies, puckering parameters[14] for these rings showed a substantial range in $\phi 2$ values (192° to 287°); θ values ranged from 3.7° to 12.9°. Puckering amplitude values were nearly constant, ranging between 0.545 Å and 0.575 Å. None of these parameters would be considered unusual.

5. Conclusions

The geometries of CDs are influenced by many factors. The original crystal structure reports describe specific

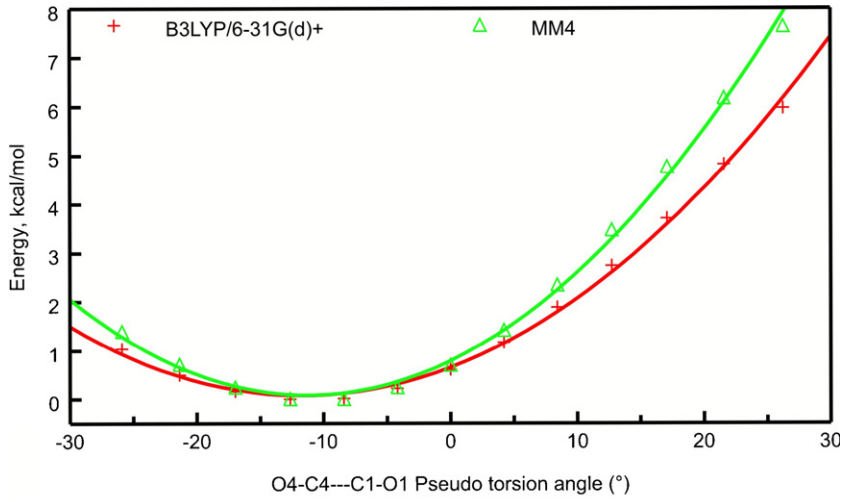

Figure 17. Relative potential energies calculated for various twists of α-D-glucopyranose with both MM4 at dielectric 1.5 and B3LYP/6-31+G(d) density functional quantum mechanics theory. The glucose had O6 in the *gg* orientation and the secondary hydroxyl groups were oriented counterclockwise; O2–H was oriented trans to H–C2. Negative values of the twist angle move O1 toward O2.

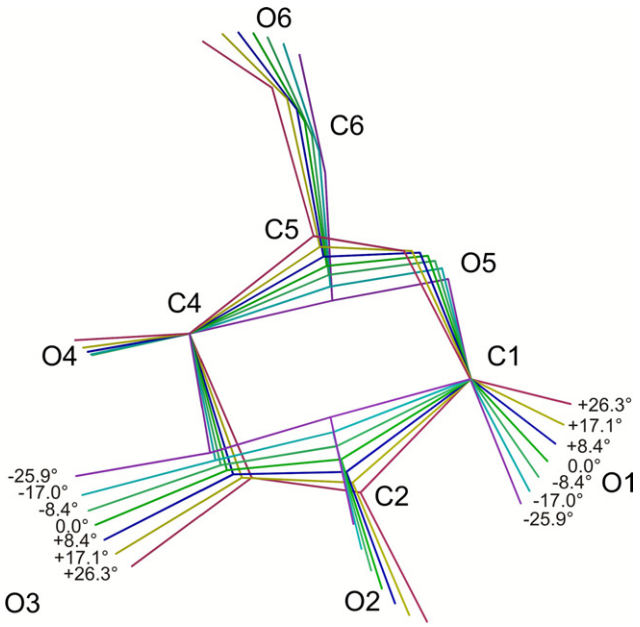

Figure 18. Structures corresponding to the B3LYP/6-31+G(d) minimized energies in Figure 17. Only every other structure is shown to reduce clutter. C4 was fixed at the origin, C1 was restricted to the *x*-axis, O4 was restricted to be in the *x*–*z* plane, and O1 was stepped in 0.1 Å intervals. As shown, the C1···C4 distance changed very little. The O4 atom did move in the *x*–*z* plane.

determinants, and reviews have also discussed some general structural principles. Here, we have focused on the intrinsic factors within or between adjacent residues. The influence discovered in the historic study[6] of the potassium acetate complex of α-CD was O3···O2′ hydrogen bonding, which results in the classic toroidal shape. Similar shapes were subsequently found for many other native CDs that have six to eight residues, and the torus or doughnut, with some modest variations, became the expected shape. However, when viewed in the context of an energy surface for a model that does not include hydrogen bonding, it appears that the hydrogen bonds stabilize what is, for the backbone atoms, a stressed shape. The average linkage conformation of classic α-, β-, and γ-CDs is distant from lower-energy shapes that would be stabilized by the *exo*-anomeric effect.

Any changes in ϕ and ψ toward that lower-energy backbone shape must, due to macrocyclic constraints, be counterbalanced by a higher-energy geometry if flipping linkages are not present. At least two factors work against flipping linkages in the α- and β-CDs. Flipping linkages apparently have higher-energy, as they are not observed in non-macrocyclic molecules, and they are in a secondary energy well on both our analog and disaccharide maps. In larger CDs, that higher-energy is a smaller part of the total energy. Secondly, the segments between observed flipping linkages have three or more glycosidic linkages and correspond roughly to a turn of a helix. In α- and β-CDs with flipping linkages there would be at least one segment with a maximum of two linkages between flipping linkages. Based on Figure 8 in the preceding paper, the minimum number of residues (or glycosidic linkages) per helix turn is about 3.5. Thus, the smaller helical segments that would be needed between flipping linkages in α- and β-CDs may not be feasible.

The β-CDs, with one more glucose residue, apparently have greater flexibility than the α-CDs. The native β-CD structures still have the general truncated cone shape with consistently elevated backbone energy but their derivatives have crumpled shapes. The derivatives have a wider range of ϕ and ψ values, and one or two linkages are within the 1-kcal/mol contour on our analog map. Of the structures examined, three derivatized β-CDs have a ring with a non-$^4C_1$ shape. Those glucopyranosyl rings have unusual and substantial positive twists, ranging from 13.8° for the $^1C_4$ ring of the permethylated β-CD to 34° in the $^OS_2$ ring in the peracetate. Some of the $^4C_1$ rings in the substituted β-CDs also have positive twists, as large as 15.9°. Those positive twists also provide right-handed character to counterbalance left-handed segments. Because the ϕ and ψ values of the butanoate are similar to those of the other substituted β-CDs, we cannot attribute the non-$^4C_1$ shapes solely to a need to compensate for the *exo*-anomeric conformation of some of the linkages. Instead, the non-$^4C_1$ shapes may be more related to substituent size. It can be observed that the β-CD with the smallest substituent, methyl, is the most elliptical or crumpled. As the substituent size increases, the CD becomes rounder, perhaps because the substituents are involved in cross-macrocycle interactions and the longer ones can reach more easily. Although still distorted, the butanoylated β-CD, with one of its own butanoyl groups inserted into its cavity, is not so crumpled that it needs a non-$^4C_1$ shape. Also, we note that of the more than 20 crystal structures that include permethylated β-CD, only one has the $^1C_4$ ring, and another (GELKEN10)[47] has an $^OS_2$ ring.

Although the lack of hydrogen bonding is clearly an important condition for the distorted shapes of acylated β-CD molecules, the proposal that their distortions arise from a tilting of glucose residues to relieve steric hindrance is probably not the only explanation. When O2′ and O3 are not hydrogen bonded to each other, they will be further apart than when they are. However, the ϕ,ψ points most distant from the average conformation are in a low-energy region favored not only by the *exo*-anomeric effect but also by the acyl stacking. That phenomenon brings the acyl groups closer together, rather than relieving a steric conflict.

Derivatized γ-CDs are the smallest molecules to incorporate flipping linkages. Their two flips allow all of the other linkages to correspond to left-handed geometries,

and energies for the non-flipping linkages are lower than the averages for the classical models. This is the beginning of a pattern that is also seen in crystalline examples of native ε-CD, CA14 and CA26, even though those molecules are hydroxyl bearing. Additional twist, apparently necessitated by the small number of residues per segment in γ-CDs, is provided by large average negative ring twists. The CAs with larger numbers of glucose residues per macroring have progressively less residue twisting, as do the α-CDs.

Amylose molecules do not have to meet the macrocycle-forming constraints that are fundamental to the CD and CA structures. On the other hand, the polymer has both crystalline and amorphous regions in the solid state. Especially in the non-crystalline zones, there may be individual situations that require substantial twisting of the polymer, including the glucose residues. Besides giving some additional insight on CD structure, this work points out the range of shapes that could be found in amylose chain segments. Also, the apparently inherent bias toward left-handed amylose helices may come partly from the negative twist seen in the average, non-macrocyclic glucose residue, as well as the preferred values of the ϕ and ψ torsion angles.

Acknowledgements

A.D.F. learned about the crystal structures of the larger CDs during a visit to Professor Wolfram Saenger's laboratory in Berlin in 1998, hosted by Dr. Katrin Gessler. Dr. Gessler also forwarded the coordinates of CA26 that were used in this work, now available from the Protein Data Bank with the code 1C58. Professor Saenger, Dr. Kazuaki Harata, and Professor Carlos Stortz kindly commented on a draft of the manuscript.

References

1. Johnson, G. P.; Stevens, E. D.; French, A. D. *Carbohydr. Res.*, in press, doi:10.1016/j.carres.2007.02.029.
2. Anibarro, M.; Gessler, K.; Uson, I.; Sheldrick, G. M.; Harata, K.; Uekama, K.; Hirayama, Fl.; Abe, Y.; Saenger, W. *J. Am. Chem. Soc.* **2001**, *123*, 11854–11862.
3. Nakagawa, T.; Ueno, K.; Kashiwa, M.; Watanabe, J. *Tetrahedron Lett.* **1994**, *35*, 1921–1924.
4. Szejtli, J. *Chem. Rev.* **1998**, *98*, 1743–1753.
5. French, D. *Adv. Carbohydr. Chem.* **1957**, *12*, 189–260.
6. Hybl, A.; Rundle, R. E.; Williams, D. E. *J. Am. Chem. Soc.* **1965**, *87*, 2779–2788.
7. Gessler, K.; Usón, I.; Takaha, T.; Krauss, N.; Smith, S. M.; Okada, S.; Sheldrick, G. M.; Saenger, W. *Proc. Natl. Acad. Sci. U.S.A.* **1999**, *96*, 4246–4251.
8. Saenger, W.; Jacob, J.; Gessler, K.; Steiner, T.; Hoffmann, D.; Sanbe, H.; Koizumi, K.; Smith, S. M.; Takaha, T. *Chem. Rev.* **1998**, *98*, 1787–1802.
9. Harata, K. *Chem. Rev.* **1998**, *98*, 1803–1827.
10. Gress, M. E.; Jeffrey, G. A. *Acta Crsytallogr., Sect. B.* **1977**, *33*, 2490–2495.
11. Takusagawa, F.; Jacobson, R. A. *Acta Crystallogr., Sect. B* **1978**, *34*, 213–218.
12. Tvaroska, T.; Bleha, T. *Adv. Carbohydr. Chem. Biochem.* **1989**, *47*, 45–123.
13. French, A. D.; Murphy, V. G. *Polymer* **1977**, *18*, 489–494.
14. Cremer, D.; Pople, J. A. *J. Am. Chem. Soc.* **1995**, *97*, 1354–1358.
15. Harata, K. *Bull. Chem. Soc. Jpn.* **1977**, *50*, 1416–1424.
16. French, A. D.; Murphy, V. G. *Carbohydr. Res.* **1973**, *27*, 391–406.
17. French, A. D.; Rowland, R. S.; Allinger, N. L. *ACS Symp. Ser.* **1990**, *430*, 120–140.
18. Jeffrey, G. A.; Huang, D.-B. *Carbohydr. Res.* **1991**, *222*, 47–55.
19. Allen, F. H. *Acta Crystallogr., Sect. B* **2002**, *58*, 380–388.
20. French, A. D.; Johnson, G. P.; Kelterer, A.-M.; Csonka, G. *Tetrahedron: Asymmetry* **2005**, *16*, 577–586.
21. Barrows, S. E.; Dulles, F. J.; Cramer, C. J.; French, A. D.; Truhlar, D. G. *Carbohydr. Res.* **1995**, *276*, 219–251.
22. French, A. D.; Johnson, G. P. *Cellulose* **2004**, *11*, 449–462.
23. Stortz, C. A. *Carbohydr. Res.* **1999**, *322*, 77–86.
24. Shimanouchi, T.; Mizushima, S.-I. *J. Chem. Phys.* **1955**, *33*, 707–711.
25. French, A. D.; Johnson, G. P. *Cellulose* **2004**, *11*, 5–22.
26. Le Bas, G.; Mason, S. A. *Acta Crystallogr., Sect. B* **1994**, *50*, 717–724.
27. Suresh, S. J.; Naik, V. M. *J. Chem. Phys.* **2000**, *113*, 9727–9732.
28. Lindner, K.; Saenger, W. *Acta Crystallogr., Sect. B* **1982**, *38*, 203–210.
29. Steiner, T.; Saenger, W. *Angew. Chem., Int. Ed.* **1998**, *37*, 3403–3407.
30. Zabel, V.; Saenger, W.; Mason, S. A. *J. Am. Chem. Soc.* **1986**, *108*, 3664–3673.
31. Steiner, T.; Mason, S. A.; Saenger, W. *J. Am. Chem. Soc.* **1990**, *112*, 6184–6190.
32. Stortz, C. A.; French, A. D. in preparation.
33. Durette, P. L.; Horton, D. *Carbohydr. Res.* **1971**, *18*, 57–80.
34. Aree, T.; Uson, I.; Schulz, B.; Reck, G.; Hoier, H.; Sheldrick, G. M.; Saenger, W. *J. Am. Chem. Soc.* **1999**, *121*, 3321–3327.
35. Steiner, T.; Saenger, W. *Angew. Chem., Int. Ed.* **1998**, *37*, 3404–3407.
36. Ding, J.; Steiner, T.; Saenger, W. *Acta Crystallogr., Sect. B* **1991**, *47*, 731–738.
37. Hinrichs, W.; Saenger, W. *J. Am. Chem. Soc.* **1990**, *112*, 2789–2796.
38. Tanase, T.; Onaka, T.; Nakagoshi, M.; Kinoshita, I.; Shibata, K.; Doe, M.; Fugi, J.; Yano, S. *Inorg. Chem.* **1999**, *38*, 3150–3159.
39. Imamura, K.; Nimz, O.; Jacob, J.; Myles, D.; Mason, S. A.; Kitamura, S.; Aree, T.; Saenger, W. *Acta Crystallogr., Sect. B* **2001**, *57*, 833–841.
40. Taga, T.; Inagaki, E.; Fujimori, Y.; Nakamura, S. *Carbohydr. Res* **1993**, *240*, 39–45.
41. Jacob, J.; Gessler, K.; Hoffmann, D.; Sanbe, H.; Koizumi, K.; Smith, S. M.; Takaha, T.; Saenger, W. *Angew. Chem., Int. Ed.* **1998**, *37*, 606–609.
42. Pangborn, W.; Langs, D.; Pérez, S. *Int. J. Biol. Macromol.* **1985**, *7*, 363–369.
43. Taga, T.; Inagaki, E.; Fujimori, Y.; Nakamura, S. *Carbohydr. Res.* **1994**, *251*, 203–212.

44. Schouten, A.; Kanters, J. A.; Kroon, J.; Looten, P.; Duflot, P.; Mathlouthi, M. *Carbohydr. Res.* **1999**, *322*, 274–278.
45. (a) Lii, J.-H.; Chen, K.-H.; Allinger, N. L. *J. Comput. Chem.* **2003**, *24*, 1504–1513; (b) Allinger, N. L.; Chen, K.-H.; Lii, J.-H.; Durkin, K. A. *J. Comput. Chem.* **2003**, *24*, 1447–1472; (c) Lii, J.-H.; Chen, K.-H.; Durkin, K. A.; Allinger, N. L. *J. Comput. Chem.* **2003**, *24*, 1473–1489; (d) Lii, J.-H.; Chen, K.-H.; Grindley, T. B.; Allinger, N. L. *J. Comput. Chem.* **2003**, *24*, 1490–1503; (e) Lii, J.-H.; Chen, K.-H.; Allinger, N. L. *J. Comput. Chem.* **2003**, *24*, 1504–1513; (f) Lii, J.-H.; Chen, K.-H.; Johnson, G. P.; French, A. D.; Allinger, N. L. *Carbohydr. Res.* **2005**, *340*, 853–862.
46. Schrödinger, 101 S. W. Main St., Suite 1300, Portland, OR, 97204.
47. Harata, K.; Hirayama, F.; Arima, H.; Uekama, K.; Miyaji, T. *J. Chem. Soc., Perkin Trans. 2* **1992**, 1159–1166.